Determining the Directional Hydraulic Conductivity of a Rock Mass

L. Mortimer[1,2], A. Aydin[3], C. T. Simmons[2] and A.J. Love[2]

[1]Hot Dry Rocks Pty Ltd, GPO Box 251, South Yarra, Victoria 3141, Australia

[2]School of Chemistry, Physics and Earth Sciences, Flinders University, GPO Box 2100, Adelaide, South Australia 5100, Australia

[3]Department of Geology and Geological Engineering, University of Mississippi, PO Box 1848, University, MS 38677, USA.

luke.mortimer@flinders.edu.au

Keywords: Fractured Rock Aquifer, Fracture Deformation, Hydraulic Conductivity, UDEC, Hydromechanical Model

ABSTRACT

The directional hydraulic conductivity of a fractured rock mass is dependent upon several factors including fracture network density, geometry, connectivity, mineralization and the effects of the contemporary *in-situ* stress field. Its estimation is critical to the numerical modelling, understanding and predictability of fluid flow within fracture networks. Directional hydraulic conductivity is typically measured directly from standard bulk hydraulic tests via the use of multiple observation wells, however, in the absence of these standard tests its estimation is problematic. This study demonstrates an alternative approach to its preliminary estimation through the use of coupled hydromechanical, discrete fracture network models constructed from the geological, hydrogeological and geomechanical characteristics of a field test site. This approach explicitly represents a deformable fracture network and the effects of the contemporary *in-situ* stress field, which allows for a more detailed evaluation of stress-dependent fracture permeability, anisotropic fluid flow and directional hydraulic conductivity trends within a fractured rock mass. These trends are depicted in terms of estimates of fracture deformation, fracture flow rates and hydraulic conductivity ellipses throughout the entire fracture network. Despite its limitations, the results of this method were found to be consistent with field observations and can provide valuable inputs for large-scale, continuum-based aquifer modelling problems and at poorly instrumented sites where sufficient number and quality of standard hydraulic tests are not available to calibrate the model.

1. INTRODUCTION

Critical to the understanding and prediction of fluid flow within any fractured rock mass is the determination of the directional hydraulic conductivity. Hydraulic conductivity (K) is a tensor, which is defined as the volume of fluid that flows through a unit area of porous/fractured media for a unit hydraulic gradient normal to that area. Within low permeability fractured rock aquifers, it is typically anisotropic in nature and governed by the inherent properties and *in-situ* stress state of the host rock and its fracture network (Hudson et al., 2005; Min et al., 2004; NRC, 1996). In particular, fluid flow is dominantly controlled by fracture network density, geometry, connectivity and mineralization whilst contemporary stress fields may superimpose a secondary influence on pre-existing fracture networks by deforming them further (NRC, 1996). An estimate of the directional hydraulic conductivity is important because it is direct input for predictive numerical models dealing with various applications ranging from shallow groundwater aquifers to deep geothermal reservoirs.

Hydraulic conductivity is a function of stress-dependant fracture permeability, which is well documented in studies of deep-seated, fractured rocks involving hydrocarbon and geothermal reservoirs as well as nuclear repositories (e.g. Gentier et al., 2000; Hillis et al., 1997; Hudson et al., 2005). In particular, *in-situ* stress fields are known to exert a significant control on fluid flow patterns in fractured rocks with a low matrix permeability. For example, in a key study of deep (>1.7 km) boreholes, Barton et al. (1995) found that permeability manifests itself as fluid flow focused along fractures favourably aligned within the *in-situ* stress field, and that if fractures are critically stressed this can impart a significant anisotropy to the permeability of a fractured rock mass. Preferential flow occurs along fractures that are oriented orthogonal to the minimum principal stress direction (due to low normal stress), or inclined ~30° to the maximum principal stress direction (due to shear dilation).

Stress-dependent fracture permeability forms as a result of the interplay between normal and shear stresses, which are the components of stress that act perpendicular and parallel to a fracture plane, respectively. In a fractured rock mass, these stresses are highly coupled and can cause fractures to deform. Fracture deformation results in changes in permeability and storage because the ability of a fracture to transmit a fluid is extremely sensitive to its aperture as demonstrated by the "Cubic Law". This law defines the bulk hydraulic conductivity of a fractured medium in the direction parallel to the fractures assuming that fractures are planar voids with two flat surfaces within an impermeable matrix (Snow, 1969). For an isolated test interval within a borehole, it is expressed as:

$$K_b = \frac{(2b)^3}{2B} \frac{\rho g}{12\mu} \qquad (1)$$

where K_b is the bulk hydraulic conductivity (m.s^{-1}) (where K_b = Transmissivity/test interval), $2b$ is the fracture aperture width (m), $2B$ is the fracture spacing (m), ρ is the fluid density (kg.m^{-3}), g is gravitational acceleration (m.s^{-2}) and μ is the dynamic viscosity of the fluid (Pa.s) (Snow, 1969).

Anisotropic flow behaviour or flow channelling is particularly strong in low fracture density and low permeability fractured rock aquifers and is best represented in numerical models through the use of coupled hydromechanical, discrete fracture network models. In contrast, standard continuum or equivalent porous media type numerical modelling methods are unlikely to account fully for anistropic flow behaviour or fracture deformation processes. The objective of this study is to demonstrate through the use of coupled hydromechanical, discrete

fracture network models how preliminary estimates of the directional hydraulic conductivity of a fractured rock aquifer maybe determined through a detailed analysis of its contemporary in-situ stress field and geological, hydrogeological and geomechanical characteristics. Although this study is based upon a shallow depth, fractured rock aquifer example the methodology described can be applied to any site at any geological or depth setting. The value of this study is that it describes the hydraulic character of a fractured rock aquifer from a multi-disciplinary approach without the need for standard borehole hydraulic tests or multiple observation wells. Furthermore, the results of this method can be used to identify potentially permeable structures as well as to estimate injection pressures and reservoir growth directions for a reservoir during hydraulic stimulation.

This study uses the Universal Distinct Element Code (UDEC) to simulate the coupled hydromechanical response of a deformable fractured rock mass and its fractures under the influence of in-situ stress fields. UDEC is a 2.5D, distinct element, discontinuum code that represents a rock mass as an assembly of discrete rigid or deformable, impermeable blocks separated by discontinuities (faults, joints etc), which are treated as boundary conditions between the blocks (Itasca, 2004). It can interpolate fully coupled hydromechanical behaviour, whereby fluid pressure and fracture conductivity is dependent upon mechanical deformation whilst simultaneously fluid pressures modify the mechanical behaviour of the fractures (Itasca, 2004). The basic fractured rock mass hydromechanical model represents the physical response and stress-displacement relationship to an imposed stress field, which satisfies the conservation of momentum and energy in its dynamic simulations with fluid flow calculations derived from Darcy's Law (for a comprehensive review of the UDEC governing equations see Itasca, 2004). In recent years, several researchers have successfully used UDEC to investigate deformation and fluid flow within fractured rock masses over a range of crustal depths, stress regimes, geological settings and fracture network geometries (e.g. Cappa et al., 2005; Gaffney et al., 2007; Min et al., 2004; Zhang and Sanderson, 1996; Zhang et al., 1996).

2. THE APPROACH TO HYDROMECHANICAL MODELLING

The approach to hydromechanical modelling involves a multidisciplinary methodology consisting of five key components, which are described as follows:

1. Determination of the in-situ stress field;
2. Geological and hydrogeological characterisation;
3. Geomechanical characterisation;
4. Hydromechanical model design and construction; and
5. Model output presentation and interpretation.

2.1 Determination of the *In-Situ* Stress Field

Stress (σ) is a tensor that describes the force per unit area at any given point within the crust. Stress fields in the crust are caused by the interplay between tectonic processes, overburden weight, depth, pore pressures and other geologic phenomenon such as volcanic activity. Stress fields are typically relatively uniform and consistent over large scale provinces (10s – 100s km) but locally perturbed in response to small-scale features such faults, intrusive bodies, significant contrasting or anisotropic rock types etc. At shallow depths (<700m) stress fields may be affected by

non-tectonic, surface related, sources of stress such as topography, thermal effects and weathering (Zoback, 2007).

The description of any *in-situ* stress field includes the relative arrangement of the three mutually orthogonal principal axes of stress referred to as the maximum (σ_1), intermediate (σ_2) and minimum (σ_3) principal axes of stress. As the Earth's surface is a free surface with zero shear stress the vertical stress (σ_V) is assumed to be one of these principal axes of stress. The other two principal axes of stress consist of the two mutually orthogonal, horizontal stress orientations referred to as the maximum and minimum horizontal principal axes of stress (σ_H and σ_h, respectively). In practice, far-field crustal stress regimes are classified using the Andersonian scheme, which relates the three major styles of faulting in the crust to the three major arrangements of the principal axes of stress (Anderson, 1951). These three major stress regimes are:

(a) normal faulting stress regime where $\sigma_V > \sigma_H > \sigma_h$;

(b) strike-slip faulting stress regime where $\sigma_H > \sigma_V > \sigma_h$; and

(c) thrust faulting stress regime where $\sigma_H > \sigma_h > \sigma_V$.

The description of the *in-situ* stress field also requires an estimate of the pore fluid pressures in the rock formation. This is important for simulating coupled hydro-mechanical behaviour (or "poroelasticity") of a fracture rock mass, which occurs when a fracture system is uniformly saturated and well interconnected and when the pore volume to rock volume ratio is small (Zoback, 2007). Pore fluid pressure (P_p) controls the deformation of a fractured rock medium as fluid pressures act to reduce the stress acting normal to a fracture plane. This altered stress state is known as the effective stress (σ') and is defined as the difference between the applied stress (σ) and the internal pore fluid pressure (Equation 2). For example, high effective stresses act to close fractures whilst low effective stresses with relatively high fluid pressures act to dilate fractures.

$$\sigma' = \sigma - P_p \qquad (2)$$

There are several techniques for measuring magnitude and directions of *in-situ* stresses, among which the following are common:

1. Overcoring and strain relief methods that involve the emplacement of strain cells in existing boreholes that measure the 3D stress state. Generally, restricted to shallow depths (<1000m).
2. Hydraulic fracturing whereby fluid is injected into a sealed-off borehole interval to induce tensile failure (often along the vertical borehole axis) of the rock providing the direct measurement of σ_3 and an estimate of σ_1 and of the stress field orientation.
3. Imaging of (vertical) borehole breakouts and drilling-induced tensile fractures which are 2D stress field indicators in the horizontal plane (i.e. σ_H and σ_h azimuths).
4. Earthquake focal mechanisms that define the far-field, regional stress regime (e.g. normal, reverse or strike-slip) and their approximate orientations. Originating at 5-20km depth, analysis of seismic wave arrival times enables sampling of large volumes of rock and are considered reliable stress field indicators if there are sufficient well-constrained measurements.
5. All of the above techniques assume that σ_V is approximately vertical and equivalent to the

integration of rock densities (overburden weight) to the depth of interest (h) and is expressed by:

$$\sigma_V = \int_0^h \rho(h).g.dh \qquad (3)$$

where $\rho(h)$ is the density as a function of depth (kg.m^{-3}), g (m.s^2) is the gravitational acceleration and h (m) is the vertical depth.

6. Pore fluid pressures are often assumed to be "hydrostatic" and equivalent to the pressure of fluid column at the depth of interest (h) expressed by:

$$P_P = \int_0^h \rho_w(h).g.dh \qquad (4)$$

where $\rho_w(h)$ is the fluid density as a function of depth (kg.m^{-3}).

However, in areas of confined fluid flow such as deep sedimentary basins pore fluid pressures can exceed hydrostatic and require direct estimates from techniques that isolate sections of formation such as drill stem tests or through the analysis of drilling mud weights.

Each stress measurement technique has its advantages and disadvantages and any stress field determinations should ideally combine as many of these techniques over the greatest depth interval possible. However, the collection of stress data is costly, time consuming and, with the exception of earthquake data, requires access to boreholes. In the absence of field data, a common practice is to use relative stress field magnitudes (i.e. ratios of $\sigma_V : \sigma_H : \sigma_h$) based upon the known stress regime determined from publicly available earthquake focal mechanism data from sources such as the World Stress Map (Heidbach et al., 2008).

2.2 Geological & Hydrogeological Characterisation

Where available, the geological context of the study site should include all information pertaining to the geological setting, lithological composition, structure, geometry, weathering, deformation history and stress path for each potential reservoir rock type. For example, if a particular sequence has been metamorphosed, multiply folded or eroded at the surface before re-burial, those events would have significant implications for permeability and joint formation within the affected rock units. Fracture network data can be obtained from a variety of sources including outcrop, drill core, borehole images as well as direct current (DC) and electromagnetic (EM) surface and borehole surveys. Of particular use are fracture scanline maps or core logs that provide important detail relating to fracture orientation, spacing, length, type, mineralisation and age relationships. Local hydrogeological data could include any reported hydraulic data from a variety of sources including well completion reports, well yields, pump tests, core permeability tests etc. This hydrogeological data compilation is beneficial as an indication of likely *in-situ* permeabilities, hydraulic gradients, flow rates and fluid chemistries that can provide useful constraints on the hydraulic conditions employed in a numerical model.

2.3 Geomechanical Characterisation

The geomechanical properties of a rock mass and fracture network are essential for modelling coupled hydromechanical processes as the elastic properties of an intact rock material together with fracture stiffness (strength) and pore fluid pressures control the amount of fracture deformation (dilation, closure and shearing) that may occur under an imposed stress field. This coupled hydromechanical behaviour occurs more strongly in low permeability, high stiffness rocks.

Important intact rock material properties include parameters such as density, bulk moduli, uniaxial compressive strength, tensile strength, cohesion and friction angle. These parameters are commonly estimated from laboratory tests such as drill core triaxial compression or ultrasonic velocity tests or from field based rock mass classifications such as those described by Hoek (2007). Furthermore, rock formations commonly contain a fabric, which may result in a mechanical anisotropy that needs to be determined and accounted for in any numerical model.

Fracture stiffness is primarily a function of fracture wall contact area. Normal stiffness (jk_n) and shear stiffness (jk_s) of a fracture are measures of resistance to deformation perpendicular and parallel to fracture walls, respectively. Normal stiffness is a critical parameter that helps to define the hydraulic conductivity of a fracture via an estimate of the mechanical aperture as opposed to the theoretical smooth planar aperture as described in the Cubic Law. Ultimately, estimates of fracture stiffness attempt to account for more realistic fracture heterogeneity, asperity contact, deformation and tortuous fluid flow. Equations 5 & 6 below describe the simplified relationship between fracture stiffness and fracture deformation (Rutqvist and Stephannson, 2002):

$$\Delta\mu_n = jk_n \, \Delta\sigma'_n \qquad (5)$$

$$\Delta\mu_s = jk_s \, \Delta\sigma_s \qquad (6)$$

which states (a) that fracture normal deformation ($\Delta\mu_n$) occurs in response to changes in effective normal stress ($\Delta\sigma'_n$) with the magnitude of opening or closure dependent upon fracture normal stiffness (jk_n); and (b) that the magnitude of shear mode displacement ($\Delta\mu_s$) depends upon the shear stiffness (jk_s) and changes in shear stress ($\Delta\sigma_s$).

Estimates of fracture stiffness are derived by a variety of field logging or laboratory tests, which are well documented in comprehensive reviews by Bandis (1993), Barton and Bandis (1985), Barton and Choubey (1977) and Hoek (2007). Standard practice is to derive stiffness estimates based upon fundamental measurements of fracture surface topography profiles and the elastic properties of the intact rock material, although these estimates are affected by many factors including:

1. Joint roughness coefficient (JRC) which is a standard measure of a fracture surface topography profile (Barton and Choubey, 1977).
2. Joint compressive strength (JCS) corresponding to the compressive strength of the fracture wall rock which can be modified by weathering and mineralization.
3. Magnitude of fracture stiffness increasing with increasing effective normal stress.
4. Fracture spacing and density and its effect on the partitioning of strain.
5. Intact rock material moduli such as Young's modulus (E), shear modulus (G), bulk modulus (K) and Poisson's ratio (ν).
6. Test type (e.g. unconfined, triaxial, *in-situ* direct shear, laboratory direct etc).
7. Sample size.

8. Definition (e.g. peak, initial or 50% during an applied test).

Fracture stiffness is probably the most difficult of all the geomechanical parameters to characterise accurately principally due to the large number of dependent variables, their heterogeneous nature and the scale dependence of key factors such as the JRC and JCS estimates. It is also often difficult to gain access to sufficient amounts of drill core or outcrop. Typically, these limitations are addressed within numerical models through the use of parameter sensitivity studies and/or geostatistical-based approaches such as, for example, Monte Carlo simulations (de Marsily, G. et al., 2005).

2.4 Hydromechanical Model Design & Construction

Dependent upon the overall objectives of the modelling exercise, the hydromechanical model is designed and constructed based upon the following considerations:

1. The conceptual rock mass and fracture network model derived from the above described characterisation stages;
2. Deterministic versus statistical based model designs;
3. Free, gradient or fixed boundary conditions for all three mechanical, stress and hydraulic states;
4. Constitutive model type for both the rock material (e.g. elastic isotropic, Mohr-Coulomb, ubiquitous joint etc) and fractures (e.g. Coulomb slip, continuously yielding, Barton-Bandis etc);
5. Model size with respect to area of interest; and
6. Computational limitations and time frame.

2.5 Model Output Presentation and Interpretation

2.5.1 Fracture Deformation Trends

To assess the effects of an imposed stress field, the amount of fracture deformation occurring across all individual fracture sets ultimately depicts the mechanical response of a fractured rock mass. For example, UDEC calculates the effective hydraulic aperture of a fracture based upon its initial fracture aperture width at zero stress plus any normal displacement (positive or negative) that has occurred as a result of deformation. This fracture deformation data can be depicted for individual fractures or fracture sets in terms of the amount of fracture closure normal to fracture walls relative to a pre-defined, initial (zero stress) reference aperture. This information is useful to evaluate any mechanical and, by corollary, hydraulic anisotropy.

2.5.2 Fracture Flow Rates

To investigate fracture network hydraulics and connectivity trends throughout a fractured rock aquifer requires an analysis of fluid flow through deformed (stressed state) vertical cross-sectional models. This process involves: (1) deforming the model under the in-situ stress field conditions; (2) fixing the final deformed model state; (3) subjecting it to steady state, fluid flow under an imposed hydraulic head gradient; and (4) evaluating the resultant fracture flow rates throughout the model. For example, UDEC estimates of fracture flow rates are derived from the Cubic Law (Equation 1) and governed by fluid pressure differentials between fracture segments whereby the flow rate in a length of a single fracture (parallel to fracture planes), subject to a pressure difference, is calculated using Darcy's Law:

$$q = \frac{(2b)^3}{12\mu} \frac{\Delta P}{L} \qquad (7)$$

Where q is the fracture flow rate (m^2.s^{-1} i.e. m^3 per 1 unit of thickness), ΔP is the pressure difference (Pa) and L is the fracture length (m).

This information is useful to assess hydraulic conductivity and connectivity trends that may occur with changes in stress, lithology or fracture network properties.

2.5.3 Hydraulic Conductivity Ellipses

The directional hydraulic conductivity of a fracture network can be determined through the estimation of 2D planar hydraulic conductivity ellipses. This process involves slicing the conceptual fracture network model into horizontal, planar depth slices chosen to capture key features such as changes in stress, lithology or fracture network properties. UDEC has previously been successfully used to estimate permeability tensors of discrete fracture network models and this study used a similar methodology whereby deformed planar models are subjected to steady-state, fluid flow under an applied hydraulic gradient across two side boundaries whilst the upper and lower boundaries act as impermeable barriers (e.g. Min et al, 2004a; Zhang et al., 1996). The effective hydraulic conductivity (K) of each model is estimated using Darcy's Law and the UDEC sum of discharge flow rates (Q) from each steady-state model whereby:

$$Q = K A i \qquad (8)$$

where Q is the sum of discharge flow rates (m^3.s^{-1}), K is the hydraulic conductivity (m.s^{-1}), A is the cross sectional area normal to the flow direction (m^2) and i is the hydraulic gradient.

To estimate the 2D hydraulic conductivity ellipse for each depth slice, the value of K is calculated for the initial fracture network model using the method described above then this entire process is repeated for 6 x 30° (i.e. 180°) horizontal rotations of the identical model. The 2D hydraulic conductivity ellipse is then constructed by plotting the value of K recorded at each 30° horizontal model rotation.

3. CASE STUDY

The field site chosen for this study is the Wendouree Winery located within the Clare Valley, South Australia. The study area is situated within the central part of the Adelaide Geosyncline, which is a Neoproterozoic to Cambrian age, thick (>10km), rift-related, sedimentary basin complex (Preiss, 2000). It is an ideal field site as it is a fractured rock aquifer terrain currently influenced by near horizontal, WNW-ESE directed compression, is seismically active and undergoing uplift and erosion (Sandiford, 2003). The Wendouree field site is located approximately 2km SSE of the township of Clare and it is a well-instrumented, multi-piezometer site located within the sub-vertical, western limb of a large syncline structure. It contains several observation wells ranging in depths from 60-222m which are all located within a low porosity and permeability, thinly laminated, carbonaceous silt and dolomite unit over an area of ~0.1 km^2 (Love, 2003). A weathered clay saprolite zone occurs from the surface with the transition to fresh rock occurring at 18m depth.

To determine the steady state, directional hydraulic conductivity and mean groundwater flow rates at

Wendouree, stochastic 2.5D UDEC hydromechanical models were constructed based upon its conceptual fracture network model and knowledge of the contemporary stress field. These models consist of 100 and 200m block size, 2D vertical cross-section and horizontal planar model slices that incorporate the effects of the 3D stress field (i.e. σ_V, σ_H, and σ_h). The philosophy of this modelling exercise is not to characterise fracture deformation modes but to demonstrate that deformation of representative, fracture network models could provide a reasonable correlation with known groundwater flow observations. These models are stochastic representations only, which are not designed to produce a precise match to the field data but to demonstrate how the process of subsurface fracture deformation alters fracture network hydraulics, connectivity and fluid flow. Therefore, some simplification of the conceptual model was necessary considering the objectives of this study, the comparatively large size of the models and the computational limitations and run time required.

3.1 Clare Valley Regional *In-Situ* Stress Field

There has been no *in-situ* borehole stress field data collected within the Clare Valley region, therefore, this study is based upon well-documented and constrained regional earthquake focal mechanism data. For example, in the year 2001 the town of Clare experienced nine small earthquakes up to a magnitude of 2.8 whilst in 1995 the nearby township of Burra recorded a significant magnitude 5.1 earthquake (Love, 1999, 2001). An evaluation of the focal mechanism for this particular Burra earthquake event revealed a reverse stress regime with near horizontal compression in a direction of 110° at a depth of 18-20km with σ_h inferred to be mutually orthogonal at 20° (D. Love, pers. comm.).Although the region is undergoing horizontal compression at depth, the upper crust is simultaneously experiencing uplift and unloading (Sandiford, 2003). Evidence found on some of the major bounding faults of the Adelaide Geosyncline suggests that the vertical component of their slip rates is in excess of tens of metres Myr^{-1} over the past 5 Myr leading to widespread uplift, erosion and the present-day topography. (Sandiford, 2003). It is not known to what depth the effects of uplift and unloading occur in this region but studies elsewhere in the world have shown that it could extend to a few hundreds of metres to 1 km below the surface (Engelder, 1985; Hancock & Engelder, 1989). As this study is focussed on the upper 200m depth horizon, a normal stress regime is employed with the hydromechanical models, to simulate isotropic, lateral relaxation of the rock mass consistent with the effects of uplift and unloading (i.e. $\sigma_V > \sigma_H = \sigma_h$). The magnitudes of stress within these models are based upon an estimate of σ_V (i.e. $\rho.g.h$) and applied as a differential stress ratio compatible with the prevailing normal stress regime (i.e. $\sigma_V > \sigma_H = \sigma_h$ at a ratio of 1: 0.5 : 0.5). The principal stress orientations used in these normal stress models are assumed to be the same as that determined for the regional reverse stress regime. This is a reasonable assumption as studies on shallow, neotectonic joint formation within sedimentary sequences found that joints related to uplift and unloading strike approximately parallel to the mean regional, maximum horizontal stress direction (Endgelder, 1985; Hancock and Engelder, 1989).

3.2 Wendouree Geological and Hydrogeological Characterisation

In-situ fractures at Wendouree were mapped using an ALT ABI140 acoustic borehole televiewer (BHTV) with a total of 626 *in-situ* fractures imaged within four observation wells ranging in depths from 90 to 222m. These fractures were subsequently analysed via stereographic projection methods, which revealed five distinct fracture sets as defined by $\geq 2\%$ data density contours, labelled sets A – E (Figures 1a & b). This BHTV fracture dataset correlates with bedding (Set A) and joint set (Sets B-E) measurements recorded from nearby outcrop and elsewhere within the Clare Valley.
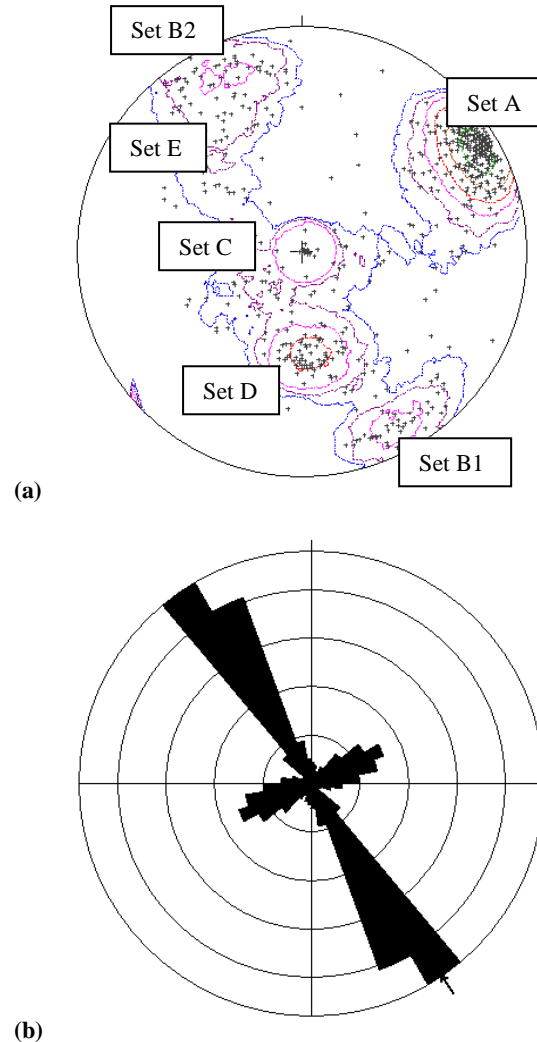

(a)

(b)

Figure 1: (a) Contoured, lower hemisphere, equal area stereonet of poles to all Wendouree BHTV-imaged fracture planes (Contours = Density/1% Stereonet Area; n = 626). (b) Corresponding Frequency-Azimuth rose diagram of all BHTV-imaged structures (Data Frequency = Azimuth). Produced with GEOrient© v9.2

Fracture parameters such as fracture trace lengths, spacings and apertures were recorded from horizontal and vertical scanline mapping data of a small, nearby outcrop (Halihan, 1999) with additional data obtained from drill core and BHTV logs. Aperture values from outcrop averaged 100-200 μm across all fracture sets but varied up to a maximum of 130mm (Halihan, 1999). This wide range in apertures is unlikely to be truly representative reflecting the effects of site disturbance by excavation, unloading and weathering. The average fracture spacing determined from the horizontal and vertical scanline maps was 0.13 and 0.16mm, respectively. However, this scanline fracture mapping dataset is only representative of one section located several metres below the surface which cannot be

extrapolated to depth. Its value lies in the detail of the relative differences between the individual fracture sets.

All of the geological data collected at Wendouree was combined to develop a conceptual fracture network model consisting of a densely fractured, clay saprolite weathered, upper zone (0-20m), a less fractured transitional zone (20-40m) and a broadly fractured lower zone (>40m) (Figure 2). With increasing depth there is a trend of decreasing fracture density based upon a reduction in the number of joint sets (Sets B, C, D & E) against a persistent background of high density bedding planes (Set A). The corresponding stochastic UDEC fracture network model consists of a bedding plane to joint set density ratio of 2:1 in the upper zone, 16:1 in the transitional zone and 32:1 in the lower zone (Table 1; Figure 3a & b). This fracture density trend was observed in the limited and vertically biased drill core and BHTV logs, however, it is an estimate only as the precise values are unknown. The primary cause of this fracture density trend is attributed to the effects of uplift and unloading. For example, the Wendouree BHTV logs revealed a proportionally greater amount of sub-horizontal joints in the upper 40m depth horizon, which is considered indicative of neotectonic joint formation in response to unloading (Hancock & Engelder, 1989). Thus, the increased development of unloading-related, sub-vertical flexural and sub-horizontal sheeting (or relaxation) joints closer to the surface creates a distinct zoning of the vertical fracture density profile throughout the entire aquifer system.
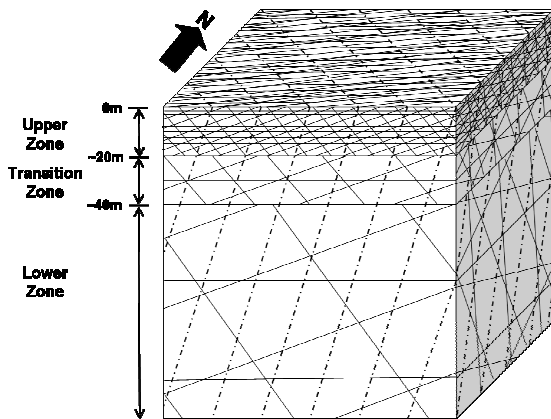

Figure 2: The Wendouree conceptual fracture network model showing decreasing joint densities between the upper, transition and lower zones. Dashed lines denote the persistent, dense, bedding planes of Set A whilst the solid lines represent joint sets B, C, D and E

As part of the hydrogeological characterisation stage, the BHTV logs were combined with high-resolution temperature logs to identify the potential hydraulic conductivity of in-situ fractures. This interpretation suggested that an anisotropic fracture permeability direction exists, which favours vertical to steeply dipping bedding planes and joints (Mortimer et. al., 2008). This interpretation is supported by another Clare Valley study, whereby several direct current (DC) and electromagnetic (EM) surface and borehole geophysical surveys found that the most significant hydraulically conductive structures were steep angle bedding planes and that the direction of maximum hydraulic conductivity is aligned with the strike of bedding (Skinner and Heinson, 2004). In addition, an analysis of piezometer pump tests, [222]Rn concentration

depth profiles as well as regional borehole groundwater yields also found that across the entire catchment groundwater flow rates decrease significantly and non-linearly with depth, particularly from 40m depth below the surface (Love, 2003; Mortimer et al., 2008).

Table 1 Mean orientation (std. dev.), trace (std.dev.), and spacing for the upper, transition and lower zones of the Wendouree stochastic UDEC models. Note that the bedding (Set A) orientation is fixed and that the NW-SE cross-section models use modified apparent dips.

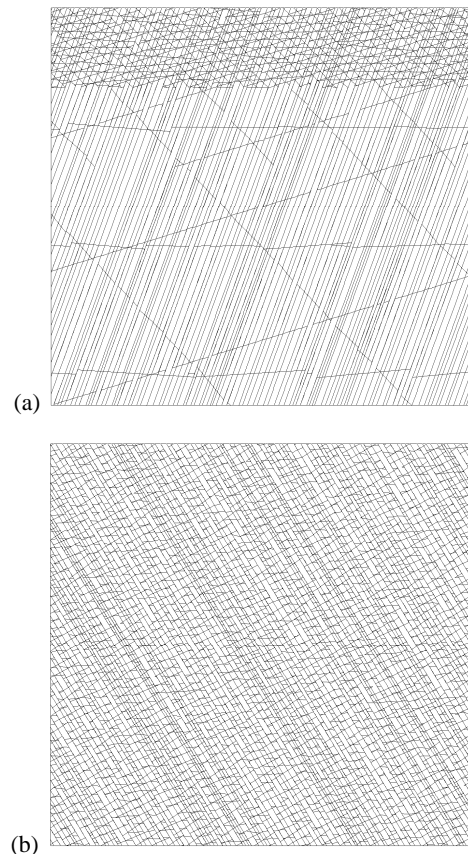| Fracture Set	Mean True Dip & Dip Direction	Mean Trace (m)	Mean Spacing (m)
A	78(0) / 240(0)	>200	0.5-1.5
B1	78(9) / 331(10)	6 (5)	2,16,32
B2	75(6) / 155(9)	6 (5)	2,16,32
C	2(6) / 013(33)	11 (18)	2,16,32
D	38(4) / 356(13)	2 (1)	2,16,32
E	54(5) / 146(9)	6 (5)	2,16,32

(a)

(b)

Figure 3: Example stochastic 2D Wendouree UDEC models: (a) the NE-SW vertical cross-section model, in the plane of joint set B, which is dominated by the dense bedding planes of Set A; and (b) the horizontal planar model, in the plane of joint set C, at 20m depth below the surface

3.3 Wendouree Geomechanical Characterisation

Average values of density, bulk modulus and Poisson's ratio for the intact rock material were obtained from ultrasonic velocity testing of several drill core samples (Table 2). These samples showed negligible mechanical anisotropy through tests conducted both parallel and perpendicular to the thinly laminated fabric. Furthermore, these data were used to estimate other parameters such as the uniaxial compressive strength (UCS), tensile strength, cohesion and friction angle through Mohr circle analysis and other empiricial relationships (Table 2). All of these rock material parameters are compatible with published values (see Waltham, 2002).

Fracture property estimates were determined from JRC distributions, intact rock material properties and comparison with published literature values (Table 2). The JRC distributions for each of the five fracture sets (Sets A – E) were determined from fracture logging of oriented drill core samples and were found to be highly variable (smooth to rough) with no obvious trends discernible for either individual fracture sets or the dataset as a whole (Figure 4). As fracture stiffness is a function of wall contact area, the jk_n for smooth planar surfaces can approximate the value of E whereas the jk_s, for perfectly matching rough surfaces, can approximate the value of G. From these relationships, estimates were derived based upon jk_n ranging from 1/2 (smooth) to 1/10 (rough) the value of E and jk_s ranging from 1/2 (smooth) to 1/10 (rough) the value of G, which are compatible with published data and those derived from empirical relationships (Table 2; Kulhawy, 1978; Norlund et. al. 1995). To reflect the highly variable JRC distributions, the range of jk_n and jk_s values were randomly populated (normal distribution) across all fractures within the model. In particular, each individual fracture within the model may consist of up to several separate segments with each segment being randomly assigned a jk_n and jk_s value. The objective of this approach is to better account for naturally occurring fracture heterogeneity such as contact area distribution, weathering, mineralisation etc and ultimately heterogeneity in stiffness along individual fracture planes. Fracture friction and dilation angle were both inferred as zero as they have only a minimal impact on the overall modelling results and are only one of many difficult parameters/uncertainties to quantify. Also, this study was not interested in studying fracture failure modes, simply relative deformation trends across the various fracture sets within the fracture network under the imposed stress field. The fracture dilation angle is critical in numerical studies investigating the role of rock mass dilation in dealing with excessive pore pressures and rock mass stability during tunnelling. However, such systems represent transient systems whereas this study is interested in modelling hydromechanical coupling in a steady state system. The initial at surface (zero stress) reference aperture was set as 0.5mm, which is considered appropriate to facilitate the observation of overall fracture network deformation patterns. This initial reference aperture state is not considered critical, as it is the relative effects of the *in-situ* stress field on individual fractures, which are the main objective.
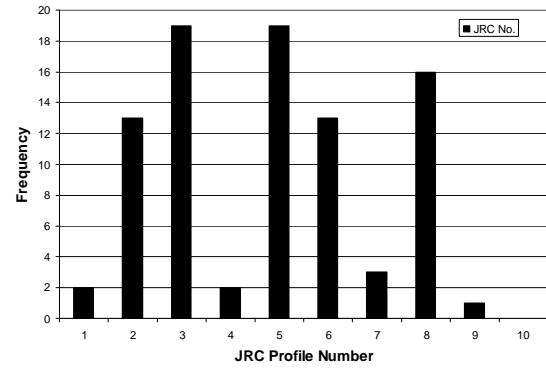

Figure 4: Frequency histogram of the JRC distribution recorded across the entire Wendouree drill core fracture dataset (Sets A – E). JRC numbers correspond to smooth (1) to rough (10) fracture surface profiles (see Barton and Choubey, 1977)

Table 2 UDEC Rock Mass and Fracture Parameters used to construct the Wendouree hydromechanical models.

UDEC Model Parameters	Value	Units
Rock Material Density (ρ)	2732	kg.m^{-3}
Poisson's Ratio (ν)	0.27	-
Young's Modulus (E)	77e6	Pa
Bulk Modulus (K)	96e9	Pa
Shear Modulus (G)	30e9	Pa
Cohesion (c)	19e6	Pa
Friction Angle (φ)	54	Degrees
Dilation Angle (ψ)	0	Degrees
Uniaxial Compressive Strength	128e6	Pa
Tensile Strength	8.5e6	Pa
Joint Normal Stiffness (jk_n)	7.7 - 35.1e9	Pa.m^{-1}
Joint Shear Stiffness (jk_s)	3.0 - 13.6e9	Pa.m^{-1}
Joint Cohesion	0	Pa
Joint Tensile Strength	0	Pa
Joint Friction Angle	0	Degrees
Joint Dilation	0	Degrees
Joint Aperture (at zero stress)	0.5	mm
Joint Residual Aperture	0.1	mm
Joint Permeability Constant	83.3	(Pa.s)$^{-1}$
Water Density (fresh @ 20°C)	1000	kg.m^{-3}

3.4 Wendouree Model Design & Construction

In these models, rock mass deformation was defined by the Mohr-Coulomb model, which is the conventional model used to represent shear failure in rocks and soils whilst fracture behaviour was defined by the Coulomb-Slip criterion, which assigns elastic stiffness, tensile strength, frictional, cohesive and dilational characteristics to a fracture (Itasca, 2004). These models defined the Earth's surface as a free surface at zero stress and pore fluid pressure with the other mechanical boundaries defined as velocity (displacement) boundaries that are either "roller" (cross-section models) or fixed (planar models). Roller boundaries set the normal velocity as zero whilst shear velocities are unconstrained, which act like frictionless rollers between the material and the boundary allowing for some limited block displacement. Similarly, *in-situ* and boundary stresses were either set as gradients (cross-section models) or fixed (planar models). Pore fluid pressures are assumed hydrostatic and commence from the field-measured water table position at 10m below the surface.

3.5 Wendouree Fracture Deformation Profile

The fracture deformation profiles of Figure 5 show a divergence in the relative amounts of fracture deformation occurring across the individual fracture sets commencing from approximately 50m depth. In particular, the rate of fracture closure with depth is approximately uniform for the moderate dipping to sub-horizontal joint sets (Sets C, D & E) whilst the steep dipping bedding planes (Set A) close at a lesser rate. Using these closure estimates, the reduction in equivalent parallel-plate hydraulic conductivities for individual fractures can be derived from the Cubic Law (Equation 1). For example, at a depth of 185m the average fracture hydraulic conductivities for the steep dipping bedding planes (Set A) and the moderate dipping to sub-horizontal joint sets (Sets C, D & E) are reduced by ~54% and ~62-71%, respectively. This progressive development with depth of an anisotropic permeability orientation along steep dipping fractures highlights the important role of fracture geometry in regards to stress-dependent fracture permeability. This result is attributed to the fact that the applied normal stress field simulates uplift and unloading through isotropic, lateral relaxation across the entire rock mass, which should result in less closure occurring along steep dipping fractures. This result is consistent with the Wendouree *in-situ* borehole fracture hydraulic conductivity and geophysical survey interpretations which both indicated that the steep dipping bedding planes are the most significant hydraulically conductive fractures (Mortimer et al., 2008; Skinner and Heinson, 2004).

3.6 Wendouree Vertical Cross-Section Flow Model

The Wendouree NE-SW cross-sectional flow model was developed by deforming the model under normal stress regime conditions before subjecting it to steady state, groundwater flow under an east to west oriented hydraulic gradient of 0.01. The UDEC model results are depicted in terms of mean fracture apertures and fracture flow rates and show that despite a uniform, linear decrease in mean fracture apertures with depth the decrease in mean fracture flow rates is non-linear (Figure 6). That is, compared to the near surface zone there is an approximately 3 fold and 7 fold decrease in mean fracture flow rates at depths of 40m and 100m, respectively. This modelled flow rate depth profile is in agreement with field measured groundwater flow profiles at Wendouree derived from flowmeter logs, piezometer pump tests and ^{222}Rn concentration depth profiles as well as from catchment-scale borehole

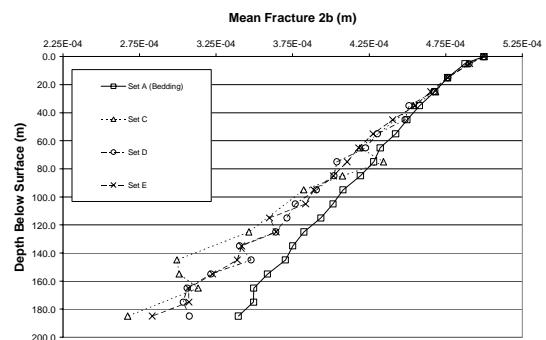groundwater yield trends (Love, 2003; Mortimer et al., 2008).

Figure 5: UDEC fracture deformation depth profiles of the individual fracture sets of the Wendouree NE-SW cross-sectional model under a normal stress regime. The initial (at surface) fracture hydraulic apertures were set at 0.5mm with data points representing the calculated mean fracture aperture for each 10m thick depth interval
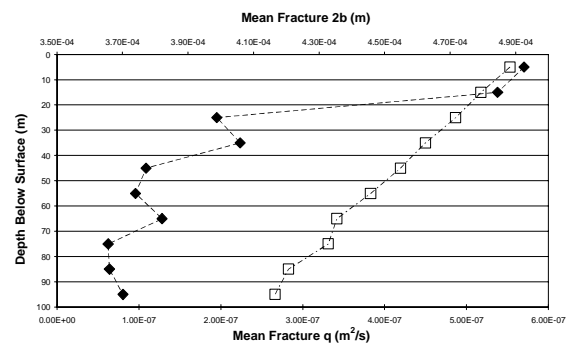
Figure 6: UDEC estimated mean fracture flow rates (diamonds, lower x-axis) and fracture apertures (squares, upper x-axis) for the Wendouree NE-SW cross-section model under a normal stress regime. The initial (at surface) fracture hydraulic apertures were set at 0.5mm

3.7 Wendouree Hydraulic Conductivity Ellipses

Horizontal planar 2D hydraulic conductivity ellipses were estimated for the Wendouree UDEC model at the 20m, 40m, 75m and 100m depth slices. Like the vertical cross-section flow model, these planar models were deformed under normal stress field conditions before being subjected to steady-state flow under an imposed east to west oriented hydraulic gradient of 0.01. The results show that at all depths the hydraulic conductivity ellipses are elongated in a WNW-ESE direction (i.e. a strike direction of 300°-120°) (Figures 7a-d). This elongation direction represents the maximum *K* direction and is slightly offset but close to the strike of the extensive, densely spaced bedding planes (Set A, 330°-150°). The NNE-SSW minimum *K* direction also approximates but is slightly offset to the strike of the less dense, finite length, joint sets (Sets B, D & E). The ellipse elongation becomes more anisotropic with depth as the ratio between the maximum versus minimum *K* axes increases, which is attributed to the lessening influence of the decreasing joint set densities against a persistent background of dense bedding planes. The overall shape of the hydraulic conductivity ellipses for these models closely

mimic those of the undeformed state suggesting that the shape and magnitude of the hydraulic conductivity ellipses are largely controlled by the original structural composition of the fracture network (i.e. fracture geometry and density) and only marginally influenced by the imposed normal stress regime. Overall, the magnitudes of the UDEC K estimates at each depth slice are in agreement with the bulk K_b estimates derived from the Wendouree piezometer pump tests (Love, 2003).
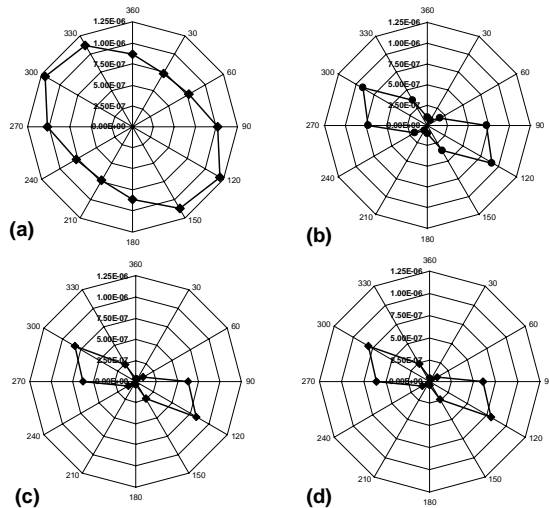

Figure 7: UDEC hydraulic conductivity (K) ellipses for the Wendouree site at (a) 20m; (b) 40m; (c) 75m and (d) 100m depth below the surface (m.s^{-1})

DISCUSSION

The above methodologies and case study describe a multidisciplinary approach to characterise and numerically model a fractured rock aquifer from structural geology and geomechanical principles. The value of this approach is that it can provide a preliminary estimate of the directional hydraulic conductivity of a fractured rock mass from outcrop or single well data with the results being reasonably comparable to those obtained from standard hydraulic tests using multiple observation wells. This methodology can also be applied to any geological or depth setting or at sites that are poorly instrumented such as, for example, deep, large scale geothermal reservoirs. The model outputs can also be used as valuable parameter inputs for larger scale continuum-based aquifer models, to identify potentially permeable structures and to estimate required injection pressures and reservoir growth directions for a reservoir during hydraulic stimulation. The results of this study also support the conclusions of previous investigations that determined that anisotropic fluid flow in fractured rock masses is dominantly controlled by the inherent properties of the fracture network whilst contemporary stress fields may superimpose a secondary influence by deforming the pre-existing fracture network further.

However, this study also identified several limitations of this approach, which are largely due to the complexities and uncertainties associated with data capture, sample representativeness and spatial confidence, particularly in regard to the geomechanical characterisation of *in-situ* rock material and fractures. Furthermore, the computational limitations and run time requirements for codes such as UDEC restrict their practical application to either detailed small-scale (<100m) studies or stochastic representations of larger scale problems. These hydromechanical models can

reflect regional scale patterns if the aquifer is homogeneous at the scale of the Representative Elementary Volume (REV). However, due to the dependence of the directional hydraulic conductivity on inherently heterogeneous properties, numerous hydromechanical models may need to be tested at various scales to ascertain its REV. To test the non-uniqueness of hydromechanical models such as these, requires a detailed parameter sensitivity analysis and, if possible, a direct comparison with field-based observations. Nonetheless, this study demonstrated that this hydromechanical modelling process can produce results that are in good agreement with direct field observations and offers an alternative preliminary approach to standard borehole hydraulic tests.

CONCLUSION

The directional hydraulic conductivity of a fracture network is dependent upon many inherently heterogeneous properties but it is critical to the understanding and predictability of fluid flow within fractured rock masses. This study has shown that preliminary estimates of the hydraulic behaviour and directional hydraulic conductivity of a fracture network can be obtained through the use of coupled hydromechanical, discrete fracture network models built upon a detailed geological, hydrogeological and geomechanical characterisation of the test site. The main advantages of this approach is that it provides an alternative method to standard borehole hydraulic tests, can be based upon outcrop or single well data, can be applied at any geological or depth setting and can account for anisotropic fluid flow by explicitly representing fractures and the effects of the *in-situ* stress field.

ACKNOWLEDGEMENTS

REFERENCES

Anderson, E. M., 1951. The dynamics of faulting and dyke formation with application to Britain. Oliver and Boyd, Edinburgh.

Barton, N.R. and Choubey, V. 1977. The shear strength of rock joints in theory and practice. Rock Mechanics, 10(1-2), 1-54.

Barton, C. A., Zoback, M. D., and Moos, D., 1995. Fluid flow along potentially active faults in crystalline rock. Geology, 23, 683-686.

Cappa, F., Guglielmi, Y., Fenart, P., Merrien-Souketchoff, V., and Thoravel, A., 2005. Hydromechanical interactions in a fractured carbonate reservoir inferred from hydraulic and mechanical measurements. International Journal of Rock Mechanics and Mining Sciences, 42, 287-306.

de Marsily, G., Delay, F., Goncalves, J., Renard, P, Teles, V. and Violette, S., 2005. Dealing with spatial heterogeneity. Hydrogeology Journal, 13, 161-183.

Engelder, T., 1985. Loading paths to joint propagation during a tectonic cycle: an example from the

Appalachian Plateau, U.S.A. Journal of Structural Geology, 7 (3/4), 459-476.

Gaffney, E. S., Damjanac, B., and Valentine, G. A., 2007. Localization of volcanic activity: 2. Effects of pre-existing structure. Earth and Planetary Science Letters, 263, 323-338.

Engelder, T., 1985. Loading paths to joint propagation during a tectonic cycle: an example from the Appalachian Plateau, U.S.A. Journal of Structural Geology, 7 (3/4), 459-476.

Gentier, S., Hopkins, D., and Riss, J., 2000. Role of Fracture Geometry in the Evolution of Flow Paths under Stress. In Faybishenko, B., Witherspoon, P.A and Benson, S.M. (eds), Dynamics of Fluids in Fractured Rocks. AGU Geophysical Monograph 122, 169-184.

Halihan, T., 1999. Clare Fracture Mapping Report, Unpublished Report, Flinders University, South Australia.

Hancock, P. L., and Engelder, T., 1989. Neotectonic joints. Geological Society of America Bulletin, 101, 1197-1208.

Hillis, R. R., Coblentz, D. D., Sandiford, M., and Zhou, S., 1997. Modelling the Contemporary Stress Field and its Implications for Hydrocarbon Exploration. Exploration Geophysics, 28, 88-93.

Hoek, E., 2007, Practical Rock Engineering. Online publication. http://www.rocscience.com/hoek/PracticalRockEngineering.asp

Hudson, J. A., Stephansson, O., and Anderson, J., 2005. Guidance on numerical modelling of thermo-hydro-mechanical coupled processes for performance assessment of radioactive waste repositories. International Journal of Rock Mechanics and Mining Sciences, 42, 850-870.

Itasca, 2004. UDEC 4.0 Theory and Background. Itasca Consulting Group Inc., Minnesota.

Kulhawy, F. H. and Goodman, R. E., 1980, Design of Foundations on Discontinuous Rock, Proceedings of the International Conference on Structural Foundations on Rock. International Society for Rock Mechanics, 1, 209-220.

Love, A. J., 2003. Groundwater flow and solute transport dynamics in a fractured rock meta-sedimentary aquifer. PhD Thesis, Flinders University, South Australia.

Min, K. B., Rutqvist, J., Tsang, C. F., and Jing, L., 2004. Stress-dependent permeability of fractured rock masses: a numerical study. International Journal of Rock Mechanics and Mining Sciences, 41, 1191-1210.

Mortimer. L., Aydin, A., Simmons, C.T. and Love, A.J., 2008. Is the In-Situ Stress Field Important to Groundwater Flow in Shallow Fractured Rock Aquifers? 2008 Western Pacific Geophysics Meeting Proceedings, American Geophysical Union.

National Research Council (NRC), 1996. Rock Fractures and Fluid Flow. Contemporary Understanding and Applications. National Academy of Sciences, Washington D.C.

Nordlund E, Radberg G, Jing L (1995) Determination of failure modes in jointed pillars by numerical modelling. In: Fractured and jointed rock masses. Balkema, Rotterdam, pp 345–350

Preiss, W. V., 2000. The Adelaide Geosyncline of South Australia, and its significance in continental reconstruction. Precambrian Research, 100, 21-63.

Sandiford, M., 2003. Neotectonics of southeastern Australia: linking the Quaternary faulting record with seismicity and in-situ stress. In Hillis, R. R. and Muller, D. (eds), Evolution and Dynamics of the Australian Plate. Geological Society of Australia, Special Publication, 22, 107-120.

Skinner, D. and Heinson, G., 2004. A comparison of electrical and electromagnetic methods for the detection of hydraulic pathways in a fractured rock aquifer, Clare Valley, South Australia. Hydrogeology Journal, 12, 576-590.

Snow, D.T., 1969. Anisotropic Permeability of Fractured Media. Water Resources Research, 5 (6), 1273-1289.

Zhang, X. and Sanderson, D. J., 1996. Numerical modelling of the effects of fault slip on fluid flow around extensional faults. Journal of Structural Geology, 18, 109-119.

Zhang, X., Sanderson, D. J., Harkness, R. M., and Last, N. C., 1996. Evaluation of the 2-D Permeability Tensor for Fractured Rock Masses. International Journal of Rock Mechanics and Mining Sciences and Geomechanical Abstracts, 33, 17-37.

Zoback, M. D., 2007, Reservoir Geomechanics. Cambridge University Press.